Supporting Information

Chemically Filled and Au-coupled $BiSbS_3$ Nanorod Heterostructures for Photoelectrocatalysis

Biplab K. Patra,[†] Santimoy Khilari,[¥] Abhijit Bera,[Γ] Shyamal K. Mehetor,[†] Debabrata Pradhan[¥] and Narayan Pradhan*[†]

[†]Department of Materials Science, [Γ]Solid State Physics, Indian Association for the Cultivation of Science, Kolkata, 700032, India

[¥] Materials Science Center, Indian Institute of Technology, Kharagpur, 721 302, India

***Half Cell Solar to Hydrogen (HC-STH) efficiency calculation*:**

The half-cell solar-to-hydrogen efficiency was measured from LSV plots recorded under illumination using following equation.[1]

$$\text{HC-STH (\%)} = J \times (V - V_{H+/H2}) \times 100(\%)/P$$

Where J represents photocurrent density, V and $V_{H+/H2}$ signifies electrode potential (vs RHE) and equilibrium redox potential of H^+/H_2 couple. The term P indicates intensity of simulated sunlight (100 mW/cm^2).

Abbreviation:

BAS = 50% Bi and 50% Sb Precursors and elemental analysis composition $Bi_{1.09}Sb_{0.91}S_3$ (Bi:Sb ~ 1:1).

Supporting Figures

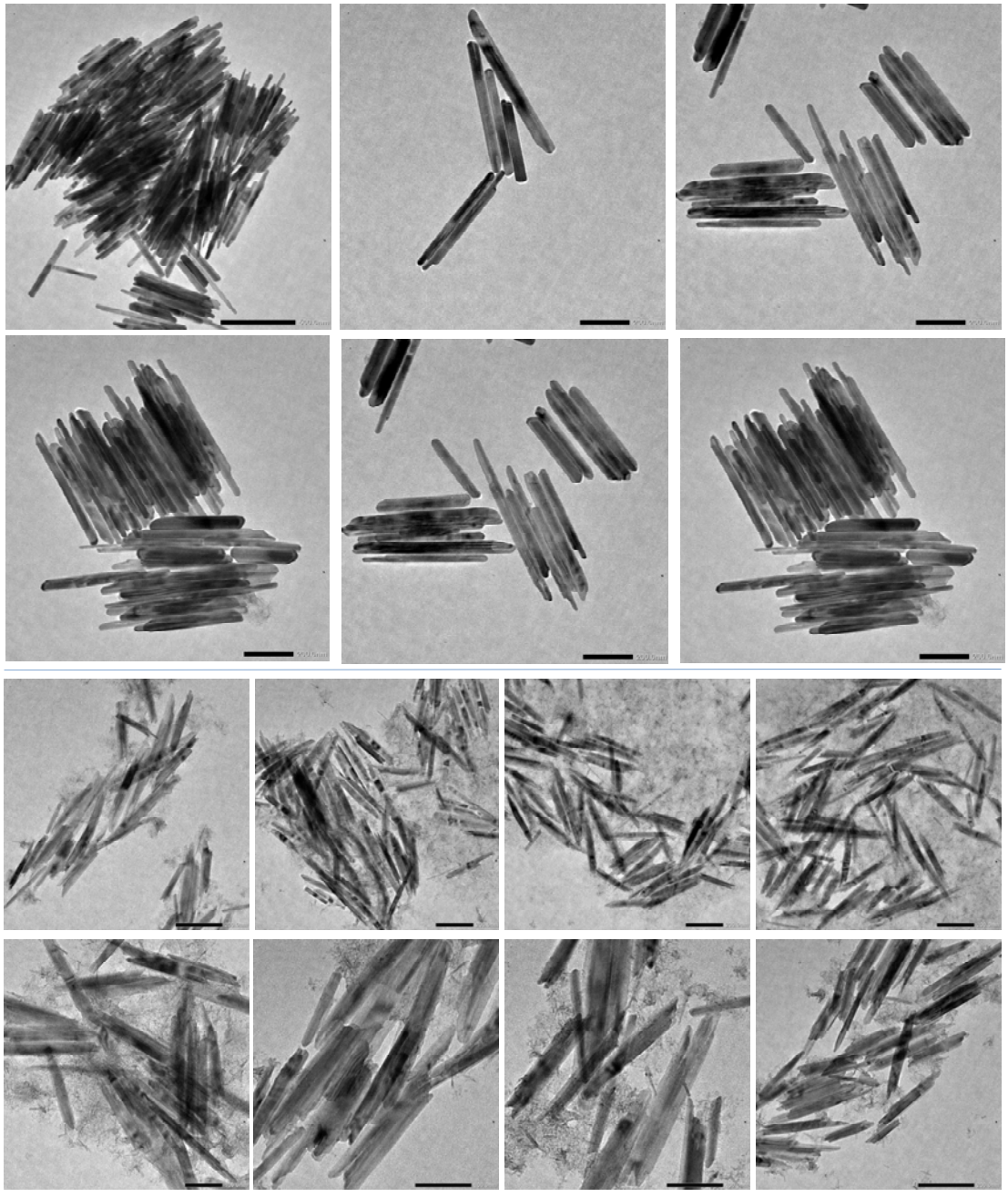

Figure S1. Top panels: TEM images of Bi_2S_3 nanotubes, obtained after 20 min of the reaction. Bottom Panels: TEM images of the sample collected at intermediate stage (30 sec) showing formation of nanotubes.

Figure S2. TEM images of Sb_2S_3 obtained under similar reaction condition of Bi_2S_3 using Sb-DDTC as precursor.

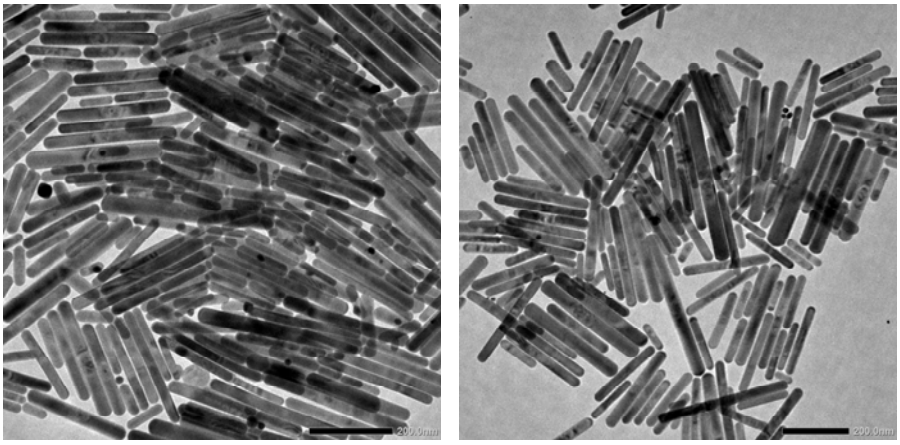

Figure S3. TEM images of $Bi_{2-x}Sb_xS_3$ obtained with Bi90% and Sb 10% precursor ratio.

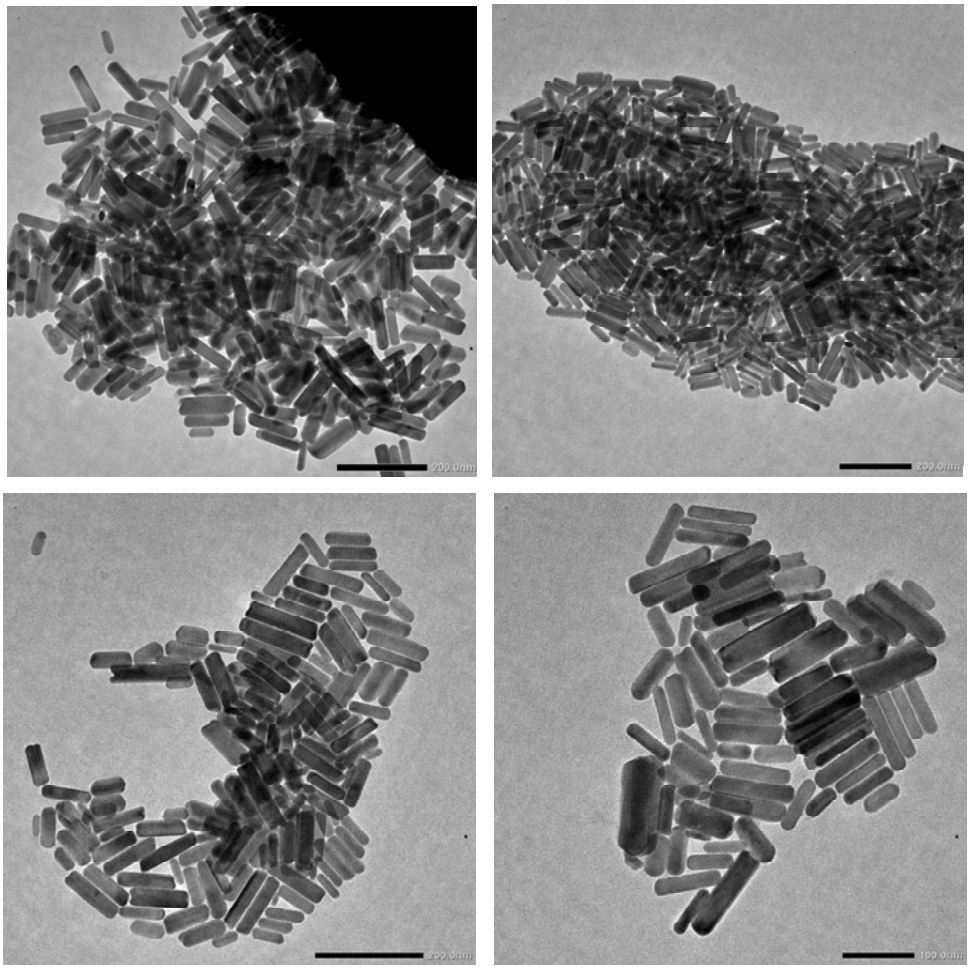

Figure S4. TEM images of BAS obtained with Bi 50% and Sb 50% precursor ratio.

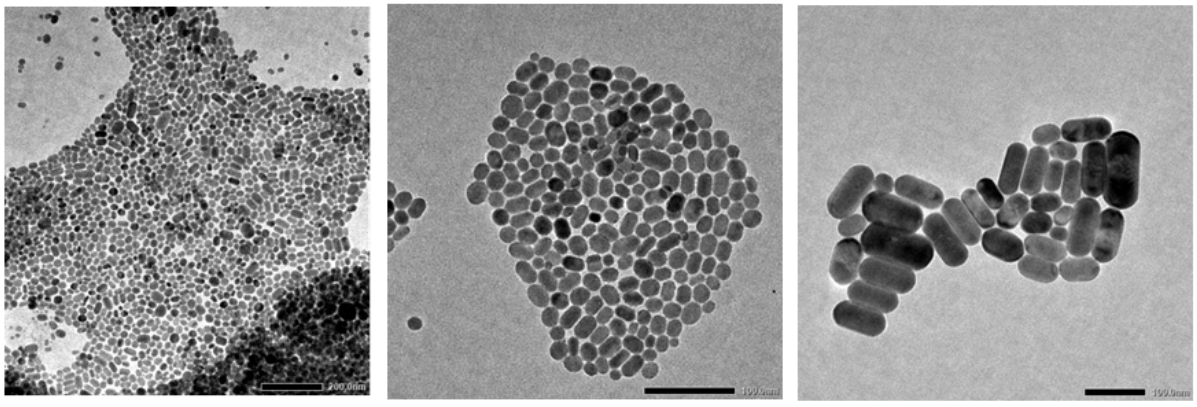

Figure S5. TEM images of Bi_{2-x} Sb_x S_3 obtained with Bi 30% and Sb 70% precursor ratio.

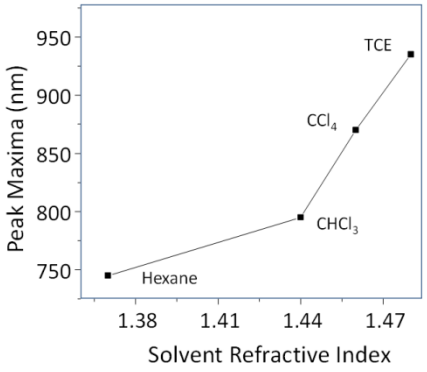

Figure S6. Plot of absorption peak maxima and solvent refractive index for BAS nanorods dispersed in different solvents.

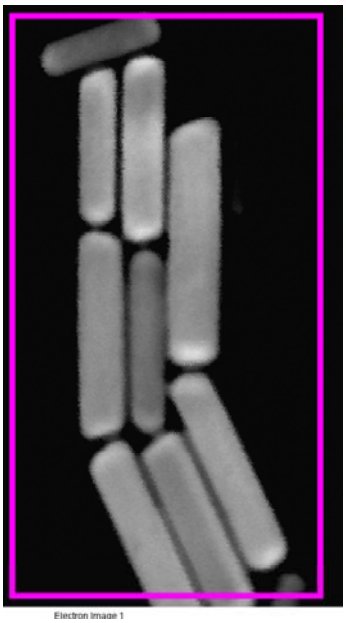

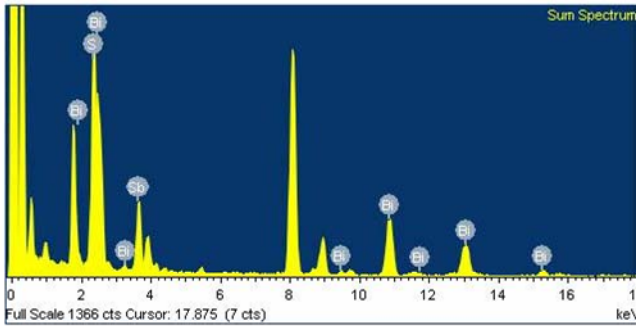

Element	Peak Area	Area Sigma	k factor	Abs Corrn.	Weight%	Weight% Sigma	Atomic%
S K	6838	226	0.940	1.000	20.78	0.67	58.06
Sb L	4363	157	1.842	1.000	25.99	0.83	19.12
Bi L	5865	178	2.806	1.000	53.23	0.97	22.81
Totals					100.00		

BAS Composition
$Bi_{1.09}Sb_{0.91}S_3$

Figure S7. EDS mapping analysis of BAS nanorods taking Bi:Sb precursors ratio 1:1. Elemental composition matches with the crystal structures of $Bi_{1.09}Sb_{0.91}S_3$.

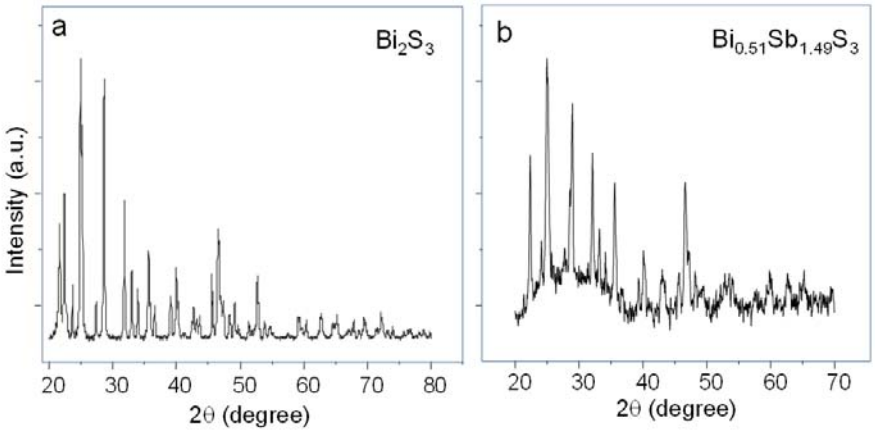

Figure S8. Powder X-ray diffraction patterns of (a) Bi_2S_3 and (b) $Bi_{0.51}Sb_{1.49}S_3$ (precursor ratio 30% Bi and 70% Sb).

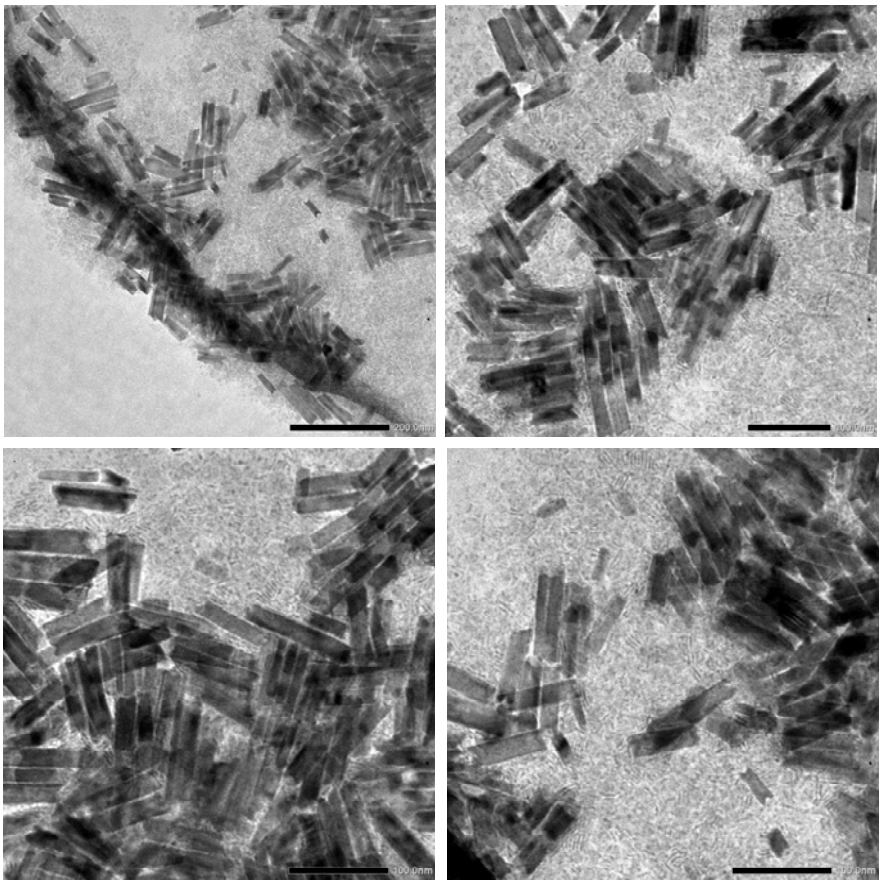

Figure S9. TEM images of BAS obtained after 1 min 30 sec of the reaction. Here Bi to Sb precursor ratio was taken 1:1.

1 min 50 sec

2 min

2 min 40 sec

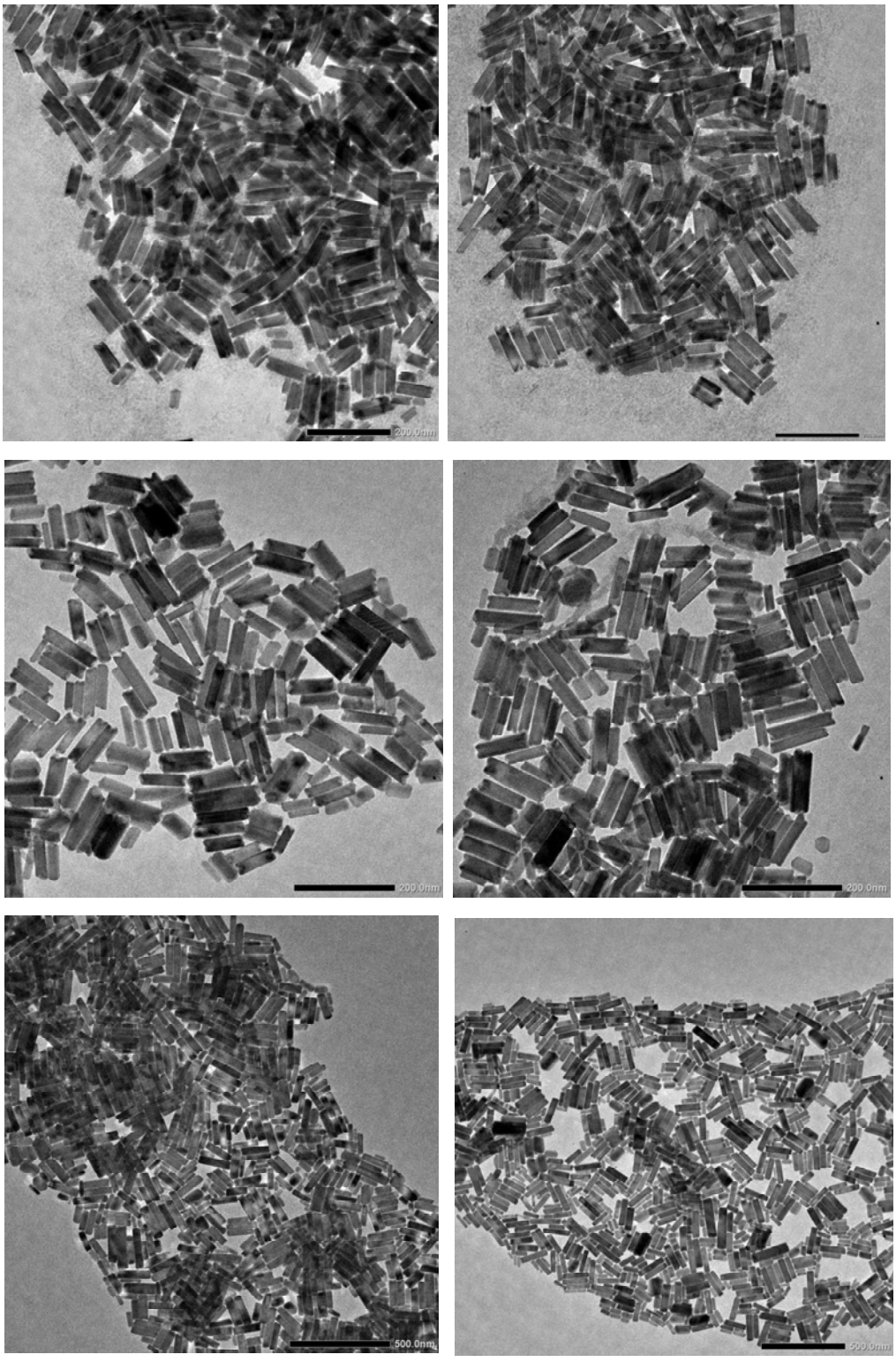

Figure S10. TEM images of BAS obtained at different time intervals from the reaction. Here Bi to Sb precursor ratio was taken 1:1.

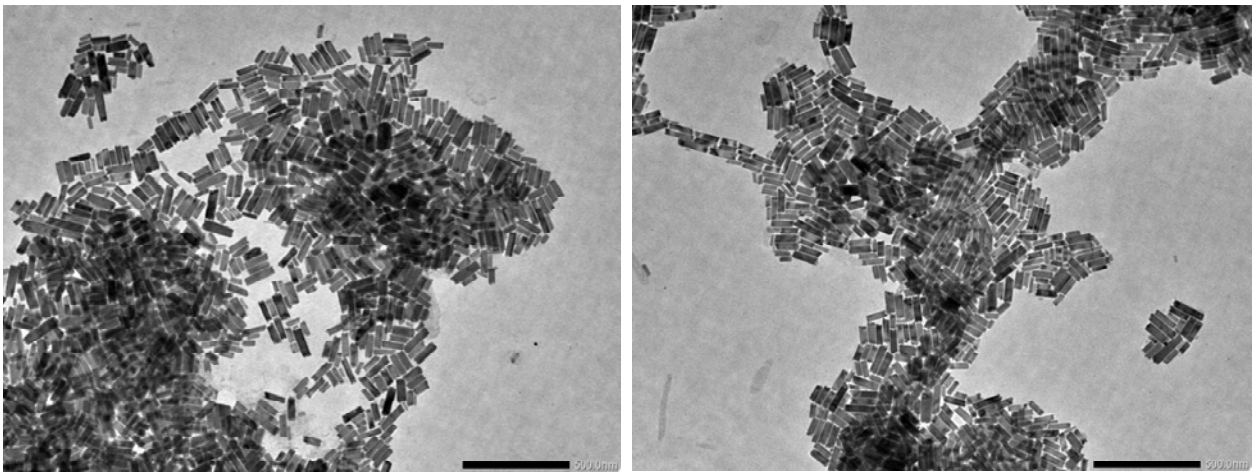

Figure S11. TEM images of BAS obtained after 3 min of the reaction. Here Bi to Sb precursor ratio was taken 1:1.

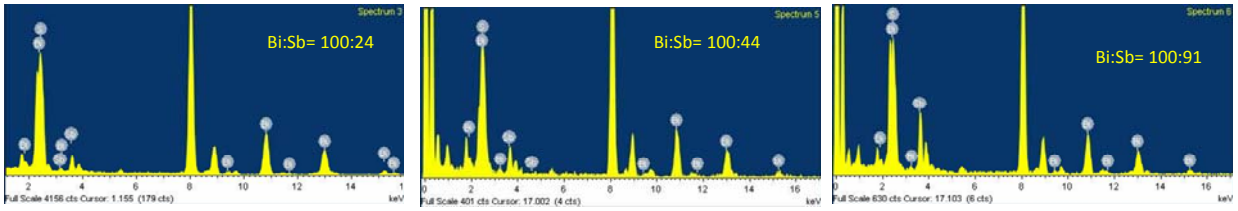

Element	Peak Area	Area Sigma	k factor	Abs Corrn.	Atomic%
S K	13464	361	0.940	1.000	52.00
Sb L	4721	194	1.842	1.000	9.41
Bi L	21811	336	2.806	1.000	38.59
Totals					100.00

Element	Peak Area	Area Sigma	k factor	Abs Corrn.	Atomic%
S K	719	131	0.940	1.000	44.02
Sb L	725	74	1.842	1.000	17.18
Bi L	2367	113	2.806	1.000	38.80
Totals					100.00

Element	Peak Area	Area Sigma	k factor	Abs Corrn.	Atomic%
S K	2962	181	0.940	1.000	51.63
Sb L	2573	123	1.842	1.000	23.14
Bi L	3160	132	2.806	1.000	25.23
Totals					100.00

Figure S12. Representative stepwise EDS spectra of BAS nanorods obtained from the washed samples collected at different time internals. (left to right 1 min 30 sec, 2 min and 5 min).

Table S1. Average Aspect Ratios in different composition mixture.

Bi_2S_3		$Bi_{1.8}Sb_{0.2}S_3$		$Bi_{1.09}Sb_{0.91}S_3$		$Bi_{0.6}Sb_{1.4}S_3$	
No of Tubes	Aspect Ratio	No of Rods	Aspect Ratio	No of Rods	Aspect Ratio	No of Rods	Aspect Ratio
6	16.6	8	7.3	6	4.9	3	2
11	15.4	5	10.5	6	4.3	5	1.4
8	15.6	5	9.5	7	5.5	6	2.1
6	14.7	4	9.1	8	4.7	12	1.4
3	14.6	3	8.4	4	5.4	6	2.0
5	13.4	6	10.7	5	4.4	5	1.5
7	14.8	2	11.4	6	4.1	7	1.6
3	15.6	6	9.3	5	4.7	7	1.5
Average = 15.0		Average = 9.5		Average = 4.7		Average = 1.6	

Table S2. **ICP AES Data**

	Sb		Bi			Sb		Bi	
Sample A Sb=70% Bi = 30%	Wt	atoms	Wt	atoms	Sample B Sb=50% Bi = 50%	Wt	No of atoms	Wt	atoms
C1	12.631	0.104	10.245	0.049	C1	27.652	0.228	44.724	0.214
C2	27.242	0.225	18.183	0.087	C2	46.342	0.383	78.375	0.375
C3	33.783	0.279	22.363	0.107	C3	57.53	0.475	109.43	0.524
Average		0.202		0.081			0.362		0.371
	(ppm)								

C1, C2 and C2 are different concentrations of samples.

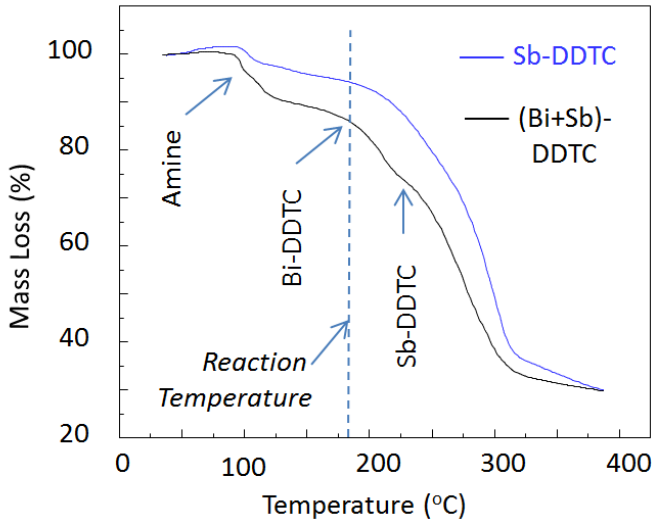

Figure S13. Thermogravimetric plot of Sb-DDTC and mixture of Bi-DDTC and Sb-DDTC in presence of octadecylamine.

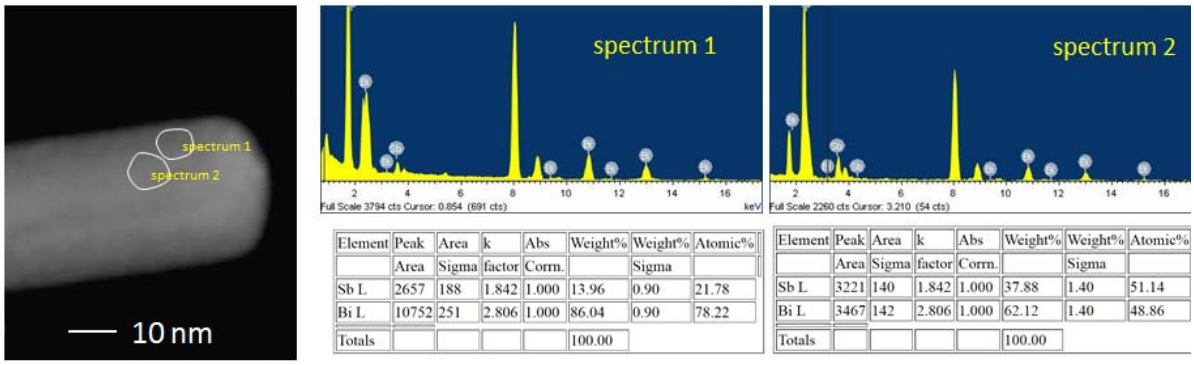

Element	Peak Area	Area Sigma	k factor	Abs Corrn.	Weight%	Weight% Sigma	Atomic%
Sb L	2657	188	1.842	1.000	13.96	0.90	21.78
Bi L	10752	251	2.806	1.000	86.04	0.90	78.22
Totals					100.00		

Element	Peak Area	Area Sigma	k factor	Abs Corrn.	Weight%	Weight% Sigma	Atomic%
Sb L	3221	140	1.842	1.000	37.88	1.40	51.14
Bi L	3467	142	2.806	1.000	62.12	1.40	48.86
Totals					100.00		

Figure 14. Left panel shows the HAADF-STEM image of a rod with marked area 1 and 2. Middle and right panel show the EDS spectra of respective area and elemental analysis.

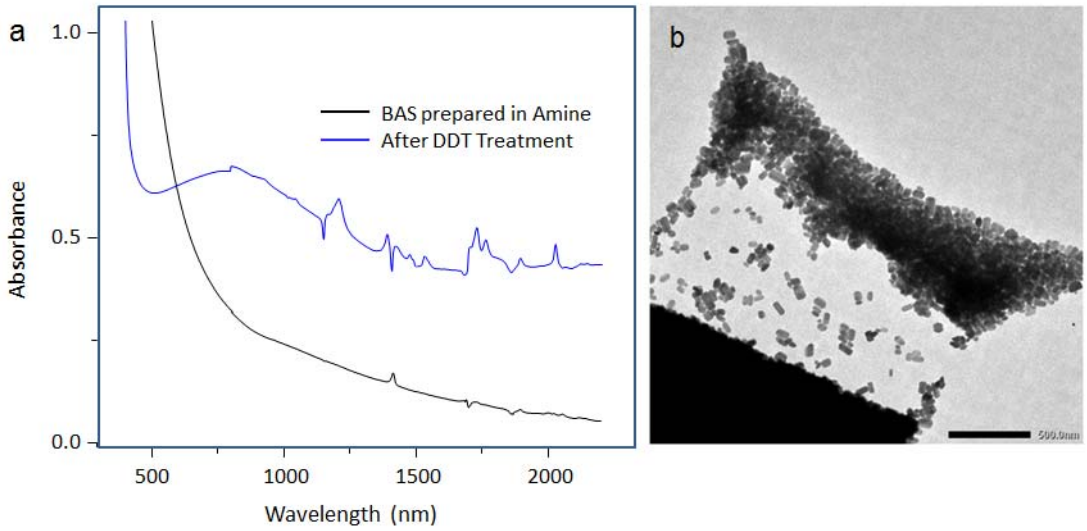

Figure S15. (a) Absorption spectra of BAS nanorods prepared in pure amine without 1-Dodecane thiol (DDT) and again after DDT treatment. LSPR obtained only after thiol treatment. (b) TEM image obtained in pure amine medium synthesis.

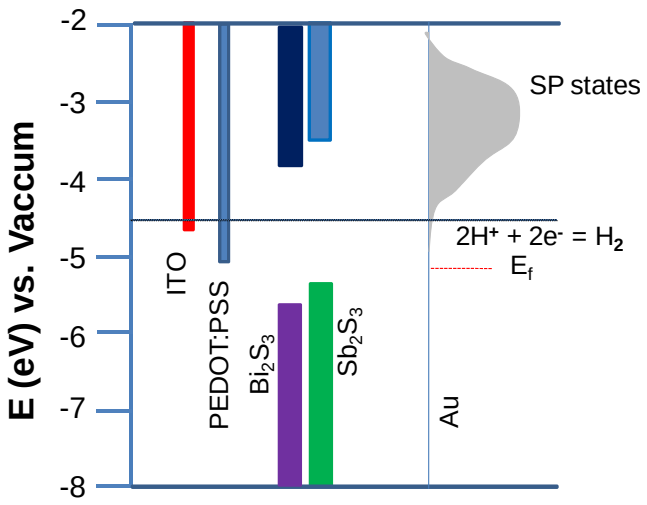

Figure S16. Band alignments of Bi_2S_3 and Sb_2S_3 along with hydrogen reduction potential.[2-3]

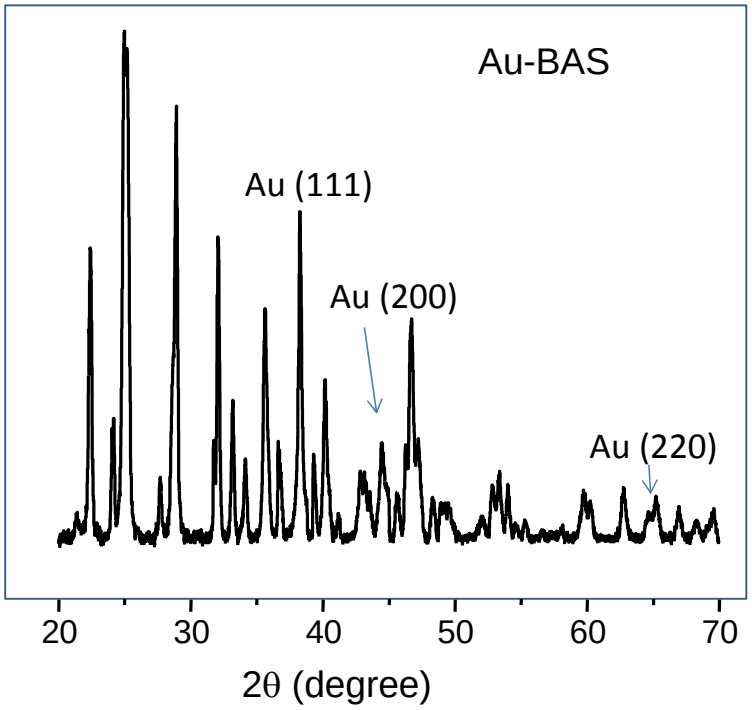

Figure S17. Powder X-ray diffraction pattern of Au-BAS nanorods.

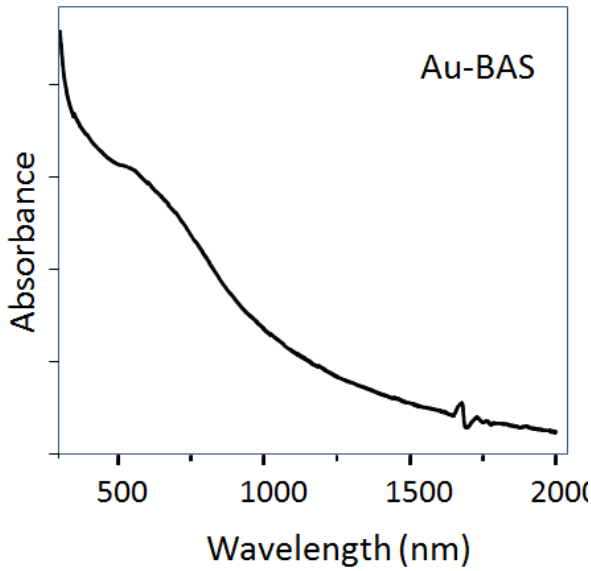

Figure S18. Absorption spectra of Au-BAS prepared in ODE dilution.

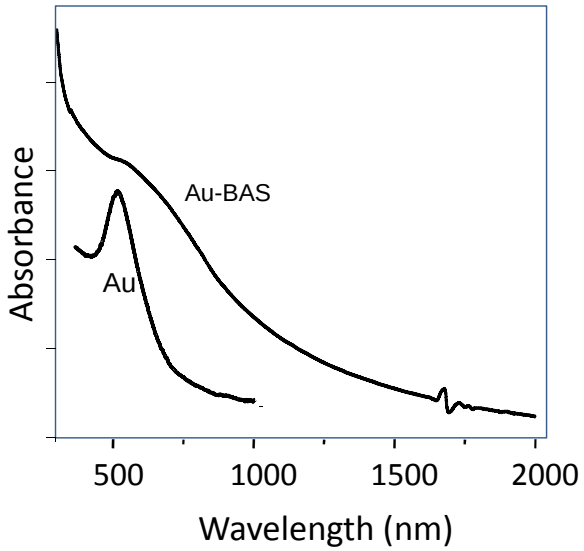

Figure S19. Absorption spectra of Au particles and Au-BAS rods. Au particles were measured in visible and Au-BAS in Near-IR spectrophotometer.

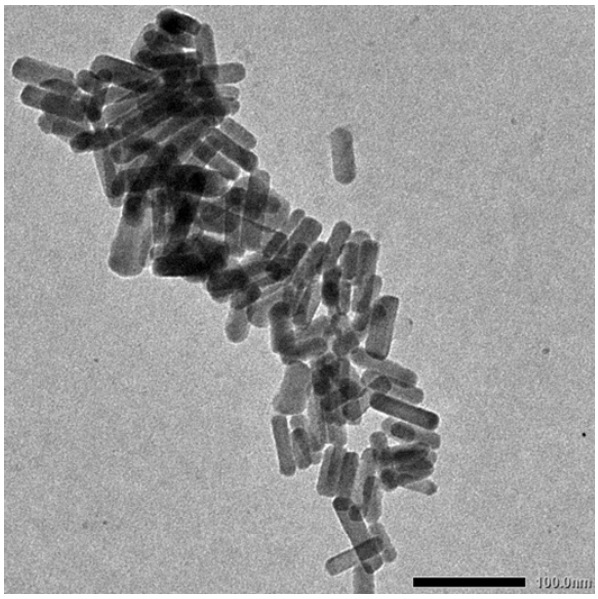

Figure S20. TEM image of BAS nanorods dispersed in water.

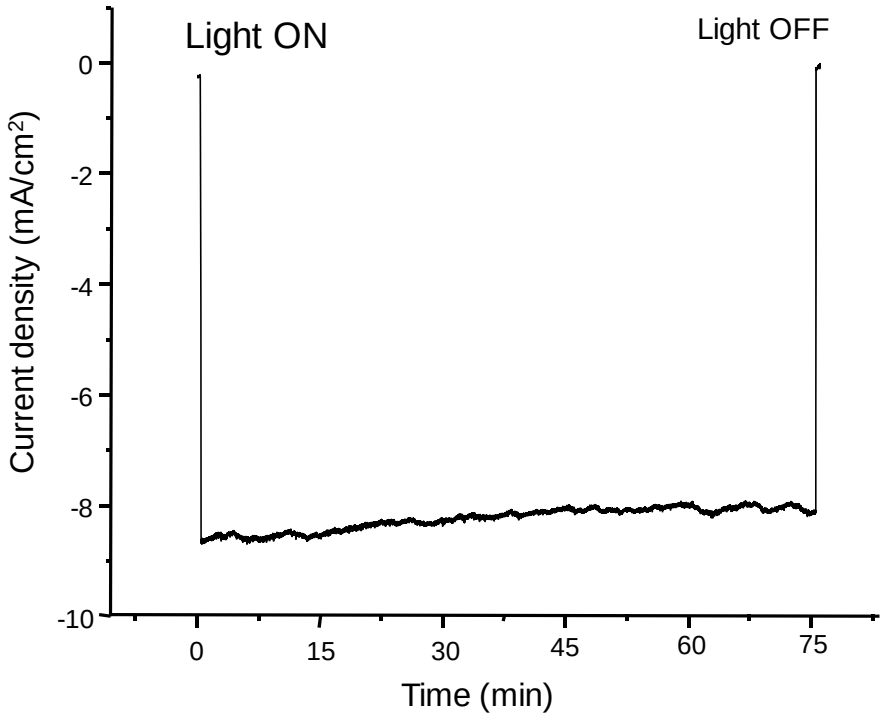

Figure S21. Stability test of photocurrent measurement under illumination switch ON/OFF mode.

Table S3: Photoelectrochemical comparison table.

Photocathode	Onset potential	Current density at 0 V vs. RHE	Reference
Pt/In_2S_3/CdS/CZTS	0.63 V vs. RHE	9.3 mA/cm^2	[4]
Pt/CdS/$CuGa_3Se_5$/(Ag,Cu)$GaSe_2$	0.62 V vs. RHE	8.79 mA/cm^2	[5]
Pt/TiO_2/CdS/$CuInS_2$	0.6 V vs. RHE	13.0 mA/cm^2	[6]
Pt/CdS/$Ag_xCu_{1-x}GaSe_2$	0.7 V vs. RHE	8.1 mA/cm^2	[7]
Pt-In_2S_3/ $CuInS_2$	0.78 V vs. RHE	15.0 mA/cm^2	[8]
Au-BAS	0.67 V vs. RHE	15.17 mA/cm^2	Present study

REFERENCES

(1) Hisatomi, T.; Kubota, J.; Domen, K., Recent Advances in Semiconductors for Photocatalytic and Photoelectrochemical Water Splitting. *Chem. Soc. Rev.* **2014,** *43*, 7520-7535.

(2) Englman, T.; Terkieltaub, E.; Etgar, L., High Open Circuit Voltage in Sb_2S_3/Metal Oxide-Based Solar Cells. *J. Phys. Chem. C* **2015,** *119*, 12904-12909.

(3) Bernechea, M.; Cao, Y.; Konstantatos, G., Size and Bandgap Tunability in Bi_2S_3 Colloidal Nanocrystals and its Effect in Solution Processed solar cells. *J. Mater. Chem. A* **2015,** *3*, 20642-20648.

(4) Jiang, F.; Gunawan; Harada, T.; Kuang, Y.; Minegishi, T.; Domen, K.; Ikeda, S., Pt/In_2S_3/CdS/Cu_2ZnSnS_4 Thin Film as an Efficient and Stable Photocathode for Water Reduction under Sunlight Radiation. *J. Am. Chem. Soc.* **2015,** *137*, 13691-13697.

(5) Zhang, L.; Minegishi, T.; Nakabayashi, M.; Suzuki, Y.; Seki, K.; Shibata, N.; Kubota, J.; Domen, K., Durable Hydrogen Evolution from Water Driven by Sunlight Using (Ag,Cu)$GaSe_2$ Photocathodes Modified with CdS and $CuGa_3Se_5$. *Chem. Sci.* **2015,** *6*, 894-901.

(6) Zhao, J.; Minegishi, T.; Zhang, L.; Zhong, M.; Gunawan; Nakabayashi, M.; Ma, G.; Hisatomi, T.; Katayama, M.; Ikeda, S.; Shibata, N.; Yamada, T.; Domen, K., Enhancement of Solar Hydrogen Evolution from Water by Surface Modification with CdS and TiO_2 on Porous $CuInS_2$ Photocathodes Prepared by an Electrodeposition-Sulfurization Method. *Angew. Chem., Int. Ed.* **2014,** *53*, 11808-11812.

(7) Zhang, L.; Minegishi, T.; Kubota, J.; Domen, K., Hydrogen Evolution from Water using $Ag_xCu_{1-x}GaSe_2$ Photocathodes under Visible Light. *Phys. Chem. Chem. Phys.* **2014,** *16*, 6167-6174.

(8) Gunawan; Septina, W.; Ikeda, S.; Harada, T.; Minegishi, T.; Domen, K.; Matsumura, M., Platinum and Indium Sulfide-modified $CuInS_2$ as Efficient Photocathodes for Photoelectrochemical Water Splitting. *Chem. Comm.* **2014,** *50*, 8941-8943.